

Published in final edited form as:

J Cardiovasc Electrophysiol. 2013 October ; 24(10): 1144–1153. doi:10.1111/jce.12176.

Apamin-Sensitive Calcium-Activated Potassium Currents in Rabbit Ventricles with Chronic Myocardial Infarction

Young Soo Lee, MD, PhD^{1,4}, Po-Cheng Chang, MD¹, Chia-Hsiang Hsueh, PhD¹, Mitsunori Maruyama, MD, PhD¹, Hyung Wook Park, MD, PhD¹, Kyoung-Suk Rhee, MD, PhD¹, Yu-Cheng Hsieh, MD, PhD¹, Changyu Shen, PhD², James N. Weiss, MD³, Zhenhui Chen, PhD¹, Shien-Fong Lin, PhD¹, and Peng-Sheng Chen, MD¹

¹Krannert Institute of Cardiology and Division of Cardiology, Department of Medicine, Indiana University School of Medicine, Indianapolis, Indiana

²Department of Biostatistics, Indiana University School of Medicine, Indianapolis, Indiana

³Cardiovascular Research Laboratory, Departments of Medicine (Cardiology) and Physiology, David Geffen School of Medicine, University of California, Los Angeles, California, USA

⁴Division of Cardiology, Department of Internal Medicine, Catholic University of Daegu School of Medicine, Daegu, Korea

Abstract

Introduction—Apamin-sensitive small-conductance calcium-activated potassium current (I_{KAS}) is increased in heart failure. It is unknown if myocardial infarction (MI) is also associated with an increase of I_{KAS} .

Methods and Results—We performed Langendorff perfusion and optical mapping in 6 normal hearts and 10 hearts with chronic (5 weeks) MI. An additional 6 normal and 10 MI hearts were used for patch clamp studies. The infarct size was 25% [95% confidence interval, 20 to 31] and the left ventricular ejection fraction was 0.5 [0.46 to 0.54]. The rabbits did not have symptoms of heart failure. The action potential duration measured to 80% repolarization (APD₈₀) in the peri-infarct zone (PZ) was 150 [142 to 159] ms, significantly ($p=0.01$) shorter than in the normal ventricles (158 to 177) ms). The intracellular Ca transient duration was also shorter in the PZ (148 [139 to 157] ms) than in normal ventricles (168 [157 to 180] ms; $P=0.017$). Apamin prolonged the APD₈₀ in PZ by 9.8 [5.5 to 14.1] %, which is greater than in normal ventricles (2.8 [1.3 to 4.3] %, $p=0.006$). Significant shortening of APD₈₀ was observed at the cessation of rapid pacing in MI but not in normal ventricles. Apamin prevented postpacing APD₈₀ shortening. Patch clamp studies showed that I_{KAS} was significantly higher in the PZ cells (2.51 [1.55 to 3.47] pA/pF, $N=17$) than in the normal cells (1.08 [0.36 to 1.80] pA/pF, $N=15$, $p=0.019$).

Conclusion—We conclude that I_{KAS} is increased in MI ventricles and contributes significantly to ventricular repolarization especially during tachycardia.

Corresponding Author: Peng-Sheng Chen, MD, 1801N. Capitol Ave, E475, Indianapolis, IN 46202. Fax: 317-962-0588, Phone: 317-962-0145, chenpp@iu.edu.

Medtronic Inc, St. Jude Inc, Cryocath Inc and Cyberonics Inc donated research equipment to Dr. Chen's laboratory. Dr. Chen is a consultant to Cyberonics Inc. Other authors: No disclosures.

Keywords

action potentials; intracellular calcium; ion channels; repolarization reserve; potassium currents; myocardial infarction

Small conductance calcium activated potassium (SK) currents are abundantly present in the neurons^{1, 2} and in atrial cardiomyocytes.³⁻⁶ However, little or no apamin-sensitive K currents are present in normal ventricles.^{3, 7, 8} These channels are activated by increases in intracellular Ca^{2+} (Ca_i) and are blocked by apamin.² In the nervous system, activation of apamin-sensitive K^+ current (I_{KAS}) is responsible for slow afterhyperpolarizations, which help terminate neuronal action potential bursts.⁹ Similar to rapid neuronal discharges, ventricular fibrillation (VF) also causes Ca_i accumulation that may persist minutes after successful defibrillation.¹⁰ Ca_i accumulation and acute postshock action potential duration (APD) shortening facilitated the development of late phase 3 early afterdepolarization (EAD)¹¹ (also known as Ca_i transient triggered firing)^{12, 13} and electrical storm in that model. The acute postshock APD shortening in failing ventricles was shown to be due to I_{KAS} activation.⁸ A more recent study by Chang et al¹⁴ showed that both the I_{KAS} and the SK protein are increased in the native hearts of transplant recipients, and that apamin significantly prolongs the APD in failing human ventricular myocytes but not in normal control ventricular myocytes. These findings suggest that I_{KAS} is important in ventricular repolarization and arrhythmogenesis in failing ventricles by shortening APD during Ca_i accumulation. However, the ability to accelerate the repolarization may also be antiarrhythmic. The redundancy in the complexities of myocardial repolarization (repolarization reserve)¹⁵ is important in maintaining normal and orderly ventricular repolarization, while reduced repolarization reserve underlies the mechanisms of afterdepolarization and ventricular arrhythmias in congenital or acquired long-QT syndromes.¹⁶ Myocardial infarction (MI) is followed by significant arrhythmogenic ion-channel remodeling including downregulation of multiple K currents in the peri-infarct zone as well as in the subendocardial Purkinje fibers.¹⁷ These changes were thought to underlie the mechanisms of afterdepolarizations and ventricular arrhythmias in MI ventricles. While K current remodeling after MI has been extensively studied, none of these studies included an evaluation of I_{KAS} after MI. If there is an increased I_{KAS} , it would counterbalance the downregulation of other K currents, hence maintaining repolarization reserve. Inhibition of I_{KAS} by apamin would prolong the APD and reduce the repolarization reserve. The purpose of the present study was to perform optical mapping studies and patch clamp studies to test the hypothesis that I_{KAS} is increased in rabbit ventricles with chronic MI and contributes significantly to ventricular repolarization in MI ventricles.

Methods

This study protocol was approved by the Institutional Animal Care and Use Committee of Indiana University School of Medicine and the Methodist Research Institute, and conforms to the Guide for the Care and Use of Laboratory Animals. New Zealand White female adult rabbits (weight 3.5–4 Kg) were used in this study (N=32). Among them, coronary artery was ligated in 20 rabbits to induce myocardial infarction (MI) and the remaining 12 rabbits were

used as normal control. MI hearts were either Langendorff perfused for optical mapping studies (N=10) or were used for patch clamp studies (N=10). The control hearts were either Langendorff perfused for optical mapping studies (N=6) or used for patch clamp studies (N=6).

Coronary artery ligation

MI was created with methods reported elsewhere.¹⁸ Left lateral thoracotomy was performed under isoflurane inhalation general anesthesia. The obtuse marginal branch of the left circumflex coronary artery or the diagonal branch of the left anterior descending coronary artery was ligated halfway between the atrioventricular groove and the cardiac apex. The limb lead electrocardiogram (ECG) was continuously monitored. MI was documented by acute ST segment elevation on ECG, purple-red discoloration and decreased wall motion distal to ligation. Left ventricular (LV) function, dimension, and mass of LV were assessed by echocardiography.

Optical Mapping

Details of optical mapping methods have been reported elsewhere.¹⁹ Briefly, the rabbits were anesthetized with sodium pentobarbital (50 mg/kg). These hearts were rapidly excised and Langendorff perfused at 25 to 30 mL/min with oxygenated Tyrode solution (in mmol/L: NaCl 125, KCl 4.5, NaHCO₃ 24, NaH₂PO₄ 1.8, CaCl₂ 1.8, MgCl₂ 0.5, and glucose 5.5) with a pH of 7.40. The hearts were stained with Rhod-2 AM (1.48 μmol/L) for Ca_i mapping and with RH237 for membrane potential (V_m) mapping. The double-stained hearts were excited with laser light at 532 nm. The fluorescence was collected and recorded with dual Complementary metal–oxide–semiconductor (CMOS) cameras (BrainVision, Tokyo, Japan) at 2 ms/frame and 100x100 pixels with a spatial resolution of 0.35x0.35 mm² per pixel. The fluorescence obtained through a common lens was separated with a dichroic mirror (650 nm cutoff wavelength), and directed to the respective camera with additional filtering (715 nm longpass for V_m and 580±20 nm for Ca_i). Optical signals were processed with both spatial (3X3 pixels Gaussian filter) and temporal (3 frames moving average) filtering. The hearts were immobilized with 20 μmol/L blebbistatin (Tocris, Ellisville, MO) during optical mapping.

Experiment Protocol

The rabbits were anesthetized 5.0 [95% CI, 4.2 to 5.9] weeks after MI. After echocardiography, the hearts were quickly removed and Langendorff perfused for optical mapping. We used 2 pacing protocols of rapid pacing during the study. Rapid pacing in non-infarcted myocardium increases Ca_i,²⁰ which activates I_{KAS} and shortens the action potential duration (APD) after pacing.⁸ In protocol I, we first measured APD to 80% repolarization (APD₈₀) at pacing cycle length (PCL) of 300 ms. We then performed S1–S2 protocol with 30 s of S1 followed by an S2 with the S1–S2 interval of 300 ms. The S1 PCL was then progressively shortened until loss of 1:1 capture. The S1–S2 coupling interval was fixed at 300 ms to minimize APD variations due to different duration of postpacing pauses. In protocol II, we paced S1 at fixed PCL of 200 ms but varied the number of paced beats (50, 100, 200, 400 beats). An S2 was then given after the last S1, with S1–S2 interval fixed at 300 ms. Apamin (100 nmol/L) was added to the perfusate for 30 minutes before the same

pacing protocols were repeated. To determine whether ATP-sensitive potassium current (I_{KATP}) activation was responsible for the APD shortening in the infarct ventricles, glibenclamide (10 $\mu\text{mol/L}$) was given before and after application of apamin in 3 infarcted ventricles.

Infarct Size Measurement

At the end of the study, the hearts (N=10) were harvested, cut horizontally into six sections and immersed in 1% triphenyl tetrazolium chloride (TTC) solution for 10 minutes. The surviving myocardium was stained brick red while infarcted was stained white.¹⁸ The percentage of MI was assessed as the ratio between the white area and total area of LV.

Rabbit Ventricular Myocyte Isolation and Patch Clamp Study

Ventricular cardiomyocytes were isolated enzymatically from left ventricles of failing rabbit hearts and whole-cell configuration of patch clamp techniques were conducted to acquire potassium currents, as previously described.⁸ Briefly, the hearts were rapidly excised and Langendorff perfused for 5 minutes with Tyrode's solution followed by perfusion with a buffer containing (in mM): NaCl, 125; MgSO₄, 1.18; KCl, 4.75; KH₂PO₄, 1.2; HEPES, 10; bovine serum albumin (BSA), 1 g/L; glucose, 10; taurine, 58.5; creatine, 24.9; EGTA, 0.02 (pH 7.4 with NaOH). This was followed by 15~20 minute perfusion with the same buffer containing 150–200 U/ml collagenase type II (Worthington, Lakewood, NJ). The hearts were removed from the perfusion apparatus; the left ventricles were cut into small pieces and dissected mechanically to obtain cardiomyocytes. Whole-cell configuration of patch-clamp technique was used to record I_{KAS} . Experiments were carried out at 36°C. Step-pulse and ramp-pulse voltages were generated with Axopatch 200B amplifier using pCLAMP-9 software (Molecular Device, Sunnyvale, CA). The data were filtered with a built-in four-pole Bessel low-pass filter (cut-off frequency: 2 kHz), and then digitized at 5 kHz. Extracellular solution contained (in mM): N-methylglucamine (NMG), 140; KCl, 4; MgCl₂, 1; glucose, 5; and HEPES, 10 (pH 7.4 with HCl). Intracellular solution contained (in mM): potassium gluconate, 144; MgCl₂, 1.15; EGTA, 1; and HEPES, 10 (pH 7.25 with KOH). To study intracellular calcium dependency of I_{KAS} , various combinations of CaCl₂ and 1 mM ethylene glycol tetraacetic acid (EGTA) were used to yield different free calcium concentrations.²¹ An online calculator (<http://www.stanford.edu/~cpatton/CaMgATPEGTA-TS.htm>) was used to calculate total CaCl₂ required to generate the desired free calcium concentrations. We used only one free calcium concentration for each pipette/cell. I_{KAS} was analyzed with Clampfit (Axon Instruments, Sunnyvale, CA), Origin 8.1 (OriginLab, Northampton, MA), and Igor software (WaveMetrics, Lake Oswego, OR).

Western Blotting

Western blotting was performed in a separate group of 5 normal control and 5 MI hearts that were not used for either mapping or patch clamp studies. 100 mg tissues were homogenized by POLY TRON in 1 ml RIPA buffer with protease inhibitor (50 mM Tris pH 8.4, 150 mM NaCl, 1% NP40, 0.5% sodium deoxycholate 1 mM PMSF, 2 $\mu\text{g/ml}$ leupeptin, 1 $\mu\text{g/ml}$ pepstatin A, and 5 $\mu\text{g/ml}$ aprotinin). Homogenates were incubated on ice for 30 minutes and then centrifuged at 14,000 rpm for 15min. 20 μg of supernatants were subjected to electrophoresis using Bio-Rad mini gel system. The separate proteins were transferred to

PVDF (Millipore). The membrane was bathed in TBS with 5% milk for one hour, and probed with either anti-KCNN2 antibody (Abcam, ab83733, 1:2500) or anti-GAPDH antibody (PIERCE, MA1-22670, 1:2500) overnight. After the interaction with primary antibody, the membrane was incubated with HRP-conjugated anti-rabbit or anti-mouse secondary antibodies (sigma, 1:5000) for 30 minutes. Finally, Luminata Crescendo HRP substrate (Millipore, WBLUR100) was added onto the membrane according to manufacturer's instruction.

Data Analysis

Optical APD₈₀ and Ca_i transient duration (Ca_iTD₈₀) were measured at 80% repolarization. Two-dimensional APD₈₀ and Ca_iTD₈₀ maps were constructed to study the spatial distribution of APD₈₀ and Ca_iTD₈₀ on epicardial surfaces of the heart. The APD₈₀ and Ca_iTD₈₀ were measured by computerized methods using all available pixels on the ventricles, excluding the atrial signals and the pixel at the edge of the ventricle. We also analyzed the relationship between preceding diastolic interval and APD₈₀ of S1 (300 ms) at each pacing cycle. *K_d* data were presented as mean and standard deviation. Continuous variables were expressed as mean and 95% confidence interval [CI].²² Paired Student's *t*-tests were used for comparison before and after apamin and glibenclamide. Independent two-sample *T* test was used to compare group means. Analyses of variance (ANOVA) with posthoc tests adjusted for multiple comparisons were used for comparison among 3 groups. All tests were performed at a 2-tailed significance level of *P* = 0.05. The statistics were computed with PASW Statistics 19 (IBM, Chicago, IL).

Results

Characteristics of MI

All rabbits developed acute ST segment elevation after coronary ligation (Figure 1A). After the heart was removed, transmural infarct (whitish scar) was visible distal to the ligation (Figure 1B). Figure 1C shows the triphenyl tetrazolium chloride (TTC) staining of the infarct ventricle, with brick red color identifying surviving myocardium and white the infarct myocardium. The estimated infarct size averaged 25 [95% CI, 20 to 31] % of the LV. None of the rabbits developed clinical signs of overt heart failure such as appetite loss, tachypnea, lethargy, ascites or pleural effusion. All MI rabbits had LV ejection fractions (EF) exceeding 45%, averaging 50 [95% CI, 46 to 54] %, which was significantly lower than baseline (62 [95% CI, 58 to 67] %, *P*=0.002). LV end-diastolic dimension, LV end-systolic dimension, and LV mass in MI rabbits were all significantly increased from baseline (baseline versus post-MI were 1.6 [95% CI, 1.5 to 1.7] cm versus 2.0 [95% CI, 1.9 to 2.2] cm, 1.1 [95% CI, 1.0 to 1.2] cm versus 1.6 [95% CI, 1.4 to 1.7] cm, 28 [95% CI, 25 to 30] g versus 37 [95% CI, 32 to 42] g, respectively, *P*<0.001 for all).

Baseline APD and Ca_iTD

Figure 2 shows APD and Ca_iTD in the normal and MI ventricles. The optical signals in the infarct zone (IZ) were too weak to be analyzed. The APD₈₀ and Ca_iTD₈₀ in the peri-infarct zone (PZ) and remote zone (RZ) were both shorter than the corresponding sites in the normal ventricles. Figure 2B shows APD₈₀ at 300 ms PCL recorded from the site marked by

an asterisk in APD₈₀ map in Figure 2A. APD₈₀ in the PZ and RZ of the MI ventricles was significantly shorter than in the normal ventricles (146 [95% CI, 138 to 159] ms, 152 [95% CI, 144 to 161] ms, versus 167 [95% CI, 158 to 177] ms, respectively, $P=0.002$ between normal and PZ, $P=0.024$ between normal and RZ). There were no significant differences in APD₈₀ between PZ and RZ ($P=0.25$). The Ca_iTD₈₀ was 148 [95% CI, 139 to 157] ms for PZ, 152 [95% CI, 143 to 161] ms for RZ, and 168 [95% CI, 157 to 180] ms for normal ventricles ($P=0.017$ between normal and PZ, $P=0.024$ between normal and RZ; Figure 2C).

Effects of Apamin on Baseline APD

Figure 3A shows APD₈₀ maps before and after apamin administration in normal and MI ventricles. Figure 3B shows corresponding optical tracings of action potentials from a single representative pixel from the site marked with asterisk in Figure 3A. While both APD₈₀ maps and the optical tracings showed that apamin prolonged APD₈₀ in normal and MI ventricles, the degree of prolongation was greater in MI than in normal ventricles. Furthermore, apamin eliminated the differences of APD₈₀ between normal and MI ventricles. Figure 3C, left panel, shows that APD₈₀ prolongation after apamin was greater in PZ (9.8 [95% CI, 5.5 to 14.1] %) and RZ (8.1 [95% CI, 4.4 to 11.7] %) than in normal ventricles (2.8 [95% CI, 1.3 to 4.3] %) ($p=0.006$ between normal and PZ, $P=0.010$ between normal and RZ). There was no difference in the degree of APD₈₀ prolongation between PZ and RZ ($P=0.469$). The right panel shows that apamin significantly increased the Ca_iTD₈₀ in normal and the MI-RZ but not MI-PZ.

Effects of Apamin on APD After the Cessation of Rapid Pacing

Progressively rapid pacing led to transiently increased Ca_i. We gave a S2 stimulus 300 ms after the last S1 and measured APD₈₀ as the difference between APD₈₀ of S2 and baseline APD₈₀ (i.e., APD₈₀ measured at 300 ms PCL). Figure 4 shows the effects of PCL on APD₈₀. Figure 4A shows examples of 300 ms PCL and 150 ms PCL in normal ventricles. The 150 ms PCL was the shortest PCL that can capture 1:1. Apamin did not increase APD₈₀ in normal ventricles, indicating no I_{KAS} activation during pacing-induced Ca_i accumulation. However, apamin significantly increased APD₈₀ in both the MI-RZ (Figure 4B) and MI-PZ (Figure 4C) of MI ventricles, especially at the shortest PCL that resulted in 1:1 capture. Figures 4D–F show the results of 3 different PCLs in normal ventricles, MI-RZ and MI-PZ, respectively. The APD₈₀ progressively increased as the PCL shortened, indicating I_{KAS} activation is progressively more important during pacing-induced Ca_i accumulation. Online Supplement Figure 1 shows the APD₈₀ as a function of the number of paced beats, while the PCL was fixed at 200 ms. Apamin significantly increased APD₈₀ in both the MI-RZ (Panel B) and MI-PZ (Panel C), but not in normal ventricles (Panel A). Online Supplement Figure 1 D–F show the results in normal ventricles, MI-RZ and MI-PZ, respectively. The APD₈₀ progressively increased as the number of paced beats increased, suggesting progressively increased importance of I_{KAS} in ventricular repolarization during tachycardia.

Effects of Glibenclamide on APD

We used glibenclamide (10 μmol/L) to block I_{KATP} , followed by apamin to block I_{KAS} ($N=3$), or vice versa ($N=3$). Figure 5A and 5B show the APD₈₀ maps. Among them, Panel A

shows results of adding glibenclamide before adding apamin. Glibenclamide did not significantly prolong APD₈₀ in these rabbits. However, after apamin administration, there was a significant global increase of APD₈₀ (Figure 5C). Figure 5B shows adding apamin before glibenclamide. Apamin administration prolonged APD₈₀ at PZ and RZ. There was no further lengthening of APD₈₀ after glibenclamide (Figure 5D).

Effects of Apamin on Conduction Velocity

The conduction velocity was measured by analyzing the wavefront propagation at 300 ms PCL. The difference of earliest and latest activation was used to determine the conduction time. The ratio between the distance traveled and the conduction time is the conduction velocity. We found that apamin significantly reduced the conduction time in MI ventricles but not in normal ventricles.

I_{KAS} in MI Ventricles Determined With Patch Clamp Techniques

Figure 6A shows representative current traces obtained with a step-pulse protocol (300 ms pulse duration; holding potential, -70 mV; see inset) in the absence and presence of 100 nmol/L apamin in the bath solution. Mean I_{KAS} density (determined as the apamin-sensitive difference current) was significantly larger in PZ of MI than in normal ventricular epicardial myocytes (I_{KAS} density at 0 mV with an intrapipette free $[Ca^{2+}]$ of 1000 nmol/L; 2.51 [95% CI, 1.55 to 3.47] pA/pF, $n=17$ cells from 10 MI rabbits, versus 1.08 [95% CI, 0.36 to 1.80] pA/pF, $n=15$ cells from 6 normal rabbits, $P=0.019$; Figure 6B). A linear mixed-effects model was fitted to the I-V curve data (Figure 6B) with a distinct cubic curve fitted to each of the three groups. There is a significant difference between Peri-MI and control, and between Peri-MI and Remote (both with p -value <0.001). There is no evidence of difference in the curve between control and Remote ($p=0.55$). Figure 6C shows the I_{KAS} current density at 0 mV recorded from epicardial cells of normal, RZ-MI and PZ-MI. There was higher I_{KAS} density in MI-PZ than normal cells. To determine the mechanism underlying increased I_{KAS} , Ca_i -dependence of I_{KAS} was studied in epicardial cells using pipette solutions containing different intracellular free $[Ca^{2+}]$. Figure 6D shows the relationship between I_{KAS} density and Ca_i . A significant difference was present at high Ca_i (1000 nM), but not at lower Ca_i . These results are consistent increased sensitivity of I_{KAS} to cytosolic Ca^{2+} in MI ventricles.

Western Blotting Analyses

The results are presented in the Online Supplement Figure 2. Although there was a trend of increased ratio between SK2 protein and the house keeping gene Glyceraldehyde-3-phosphate dehydrogenase (GAPDH) protein in PZ (1.194 [95% CI, 0.522 to 1.871]) and RZ (1.162 [95% CI, 0.334 to 1.990] versus control (0.784 [95% CI, 0.028 to 1.540])), the difference was not statistically significant ($p=0.913$).

Discussion

We found in the present study that chronic MI is associated with a significantly increased I_{KAS} density and altered I_{KAS} sensitivity to Ca_i . I_{KAS} contributes significantly to ventricular repolarization in MI ventricles.

Apamin as a Selective SK Channel Blocker

Apamin is a highly selective SK channel blocker.^{23,22} It blocks SK but no other classes of K channels.²⁴ Even among the SK channels, apamin only selectively blocks SK2 and SK3. It does not block SK1 at 100 nM,²⁴ the concentration used in the present study. Due to its subtype selectivity, we have used the term I_{KAS} rather than $I_{K(Ca)}$ to describe the K current that is blocked by apamin. The only other current known to be blocked by apamin is the fetal L-type Ca^{2+} current.²⁵ Blocking that inward current should not prolong the APD as observed in the present study. The I–V curve of I_{KAS} in this study and in the report by Xu et al³ showed inward rectification, which is the intrinsic properties of SK channels independent of intracellular blockers.²⁶ However, we do not have our own data to rule out the possibility that apamin inhibit other ionic currents in cardiac cells. Even if present, the importance of that ionic current in cardiac repolarization is probably small in normal ventricles, as the APD did not lengthen significantly in normal ventricles after apamin administration.⁸ Most of the known cardiac K currents (including the delayed rectifier K currents) are downregulated in HF and MI.²⁷ Therefore, the apamin-induced APD prolongation in failing ventricles⁸ and in MI ventricles cannot be explained by blocking the already downregulated K currents. We propose that apamin has sufficient specificity to support the conclusion of the study.

I_{KAS} and Ventricular APD in Chronic MI

In rabbit model, chronic MI is associated with time-dependent shortening of APD. The maximal shortening occurs within 30 minutes after MI, and gradually recovers to near normal values 60 days after MI.²⁸ The MI-induced APD changes are highly heterogeneous and are usually attributed to the non-uniform distribution and remodeling of ionic currents.¹⁷ However, none of the previous studies reported that MI results in an increased I_{KAS} . In the present study, we documented that I_{KAS} is increased in the rabbit model of chronic MI. Because rapid pacing increases Ca_i in non-infarcted myocardium,²⁰ the effects of apamin on APD is most pronounced during rapid pacing. In addition to blocking SK currents, apamin is also known to block $I_{Ca,L}$.²⁵ However, $I_{Ca,L}$ blocking effects of apamin should shorten, rather than lengthen, the APD.

The causes of APD change after MI are complex and likely to involve remodeling of many ion channels and Ca cycling elements. Some of these changes are likely to prolong and others to shorten APD. Our results with apamin suggest the SK channel current is part of the mix of remodeling of outward currents tending to shorten APD, and if blocked, restores APD back to a similar value as in normal tissue. These findings do not imply that the enhancement of the SK current is the only change in the surviving myocardium after MI; rather, the other changes tend to balance each other out as far as APD is concerned, and I_{KAS} merely tips the balance toward APD shortening.

I_{KAS} in MI and HF

Chua et al⁸ previously reported increased I_{KAS} in a rabbit model of pacing-induced HF. That finding was independently confirmed in a canine model of pacing-induced HF.²⁹ Furthermore, the ventricles from failing native hearts of human transplant recipients showed both increased I_{KAS} and SK2 protein levels as compared with non-failing control

ventricles.¹⁴ In the present study, the size of the MI is insufficiently large to cause significant HF symptoms. However, APD prolonged significantly after apamin administration. These findings suggest that I_{KAS} contributes significantly to the repolarization reserve of both MI and HF. In both models, conditions associated with Ca_i accumulation (prolonged rapid pacing) further magnified the APD-prolonging effects of apamin. Both models showed increased I_{KAS} sensitivity to Ca_i . The mechanisms by which diseases cause significant increased I_{KAS} sensitivity to Ca_i remain incompletely understood.

I_{KAS} and Cardiac Arrhythmias

Because rapid pacing and VF induce Ca_i accumulation,¹⁰ there is increased importance of Ca_i dynamics³⁰ and I_{KAS} ⁸ in arrhythmogenesis during tachycardia and immediately after successful defibrillation, when Ca_i handling continues to be abnormal.¹⁰ Activation of I_{KAS} in failing ventricles during rapid pacing steepens the APD restitution curve³¹ and shortens postshock APD, leading to recurrent VF.^{8, 32} Apamin flattens the restitution curve and prolongs postshock APD; both actions help suppresses VF recurrences. We showed in the present study that there is significant I_{KAS} in ventricles with chronic MI, especially during rapid pacing. While we did not observe spontaneous recurrences of VF in these non-failing ventricles, the increased I_{KAS} may still contribute to the ventricular arrhythmogenesis through its effects on APD response during rapid pacing and tachycardia. An additional proarrhythmic mechanism of I_{KAS} is the heterogeneous distribution of this ionic current. The cells in the midmyocardial layer have smaller I_{KAS} than cells in the epicardium.^{8, 14} The heterogeneous distribution of this repolarizing current in failing and infarcted ventricles may contribute to arrhythmogenesis, especially when the ventricles are exposed to drugs that block this ion current.

Clinical Implications

K currents are vital for cardiac repolarization. Downregulation of the K currents in HF and MI is thought to contribute significantly to reduced repolarization reserve that promotes afterdepolarizations, ventricular arrhythmias and sudden death,¹⁶ and the compensatory up-regulation of I_{KAS} in HF and MI can help to preserve ventricular repolarization reserve. However, the antiarrhythmic effect may be offset by excessive I_{KAS} up-regulation that shortens the APD under conditions of elevated Ca_i , leading to increased late phase 3 EAD and recurrent VF. Therefore, similar to other K channel blockers, our data suggest that I_{KAS} blockers can be both proarrhythmic and antiarrhythmic depending on the clinical situations and disease status. A second clinical implication is that, because I_{KAS} is increased in diseased ventricles, I_{KAS} blockers should not be considered as atrial selective antiarrhythmic agents in these ventricles.

Study limitation

The number of animals and cells studied is small. We tested only a single time point after MI. Whether or not I_{KAS} is increased at other time points after MI remains unknown. Because of the poor optical signals over the infarcted or ischemic regions, we were not able to study the effects of apamin on APD over the epicardial border zone (i.e., several layers of muscle fibers that survive on the epicardium over infarcted myocardium).³³ Whether or not there is I_{KAS} upregulation over epicardial border zone cells remains unclear. We used

commercially available antibody for the Western blot analyses of SK2 proteins. The sensitivity and specificity of those antibodies against SK2 protein in rabbit ventricles are unclear. While rapid pacing increases Ca_i ,²⁰ it may also have effects on restitution of other channels, redox changes and having metabolic effects. Whether or not these additional factors contributed to I_{KAS} activation during rapid rates remain unclear.

Supplementary Material

Refer to Web version on PubMed Central for supplementary material.

Acknowledgments

This study was supported in part by National Institutes of Health grants P01 HL78931, R01 HL78932, R01 71140 and R21 HL106554; and by the Laubisch and Kawata Endowments of the University of California Los Angeles (Dr. J. Weiss), a Medtronic-Zipes Endowment of Indiana University (Dr. P. Chen) and the Indiana University Health-Indiana University School of Medicine Strategic Research Initiative.

We thank Nicole Courtney and Jian Tan for their assistance.

References

1. Kohler M, Hirschberg B, Bond CT, Kinzie JM, Marrion NV, Maylie J, Adelman JP. Small-conductance, calcium-activated potassium channels from mammalian brain. *Science*. 1996; 273:1709–1714. [PubMed: 8781233]
2. Adelman JP, Maylie J, Sah P. Small-conductance Ca^{2+} -activated K^{+} channels: Form and function. *Annu Rev Physiol*. 2011
3. Xu Y, Tuteja D, Zhang Z, Xu D, Zhang Y, Rodriguez J, Nie L, Tuxson HR, Young JN, Glatter KA, Vazquez AE, Yamoah EN, Chiamvimonvat N. Molecular identification and functional roles of a Ca^{2+} -activated K^{+} channel in human and mouse hearts. *J Biol Chem*. 2003; 278:49085–49094. [PubMed: 13679367]
4. Tuteja D, Xu D, Timofeyev V, Lu L, Sharma D, Zhang Z, Xu Y, Nie L, Vazquez AE, Young JN, Glatter KA, Chiamvimonvat N. Differential expression of small-conductance Ca^{2+} -activated K^{+} channels sk1, sk2, and sk3 in mouse atrial and ventricular myocytes. *Am J Physiol Heart Circ Physiol*. 2005; 289:H2714–2723. [PubMed: 16055520]
5. Li N, Timofeyev V, Tuteja D, Xu D, Lu L, Zhang Q, Zhang Z, Singapuri A, Albert TR, Rajagopal AV, Bond CT, Periasamy M, Adelman J, Chiamvimonvat N. Ablation of a Ca^{2+} -activated K^{+} channel (sk2 channel) results in action potential prolongation in atrial myocytes and atrial fibrillation. *J Physiol*. 2009; 587:1087–1100. [PubMed: 19139040]
6. Tuteja D, Rafizadeh S, Timofeyev V, Wang S, Zhang Z, Li N, Mateo RK, Singapuri A, Young JN, Knowlton AA, Chiamvimonvat N. Cardiac small conductance Ca^{2+} -activated K^{+} channel subunits form heteromultimers via the coiled-coil domains in the c termini of the channels. *Circ Res*. 2010; 107:851–859. [PubMed: 20689065]
7. Nagy N, Szuts V, Horvath Z, Seprenyi G, Farkas AS, Acsai K, Prorok J, Bitay M, Kun A, Pataricza J, Papp JG, Nanasi PP, Varro A, Toth A. Does small-conductance calcium-activated potassium channel contribute to cardiac repolarization? *J Mol Cell Cardiol*. 2009; 47:656–663. [PubMed: 19632238]
8. Chua SK, Chang PC, Maruyama M, Turker I, Shinohara T, Shen MJ, Chen Z, Shen C, Rubart-von der Lohe M, Lopshire JC, Ogawa M, Weiss JN, Lin SF, Ai T, Chen PS. Small-conductance calcium-activated potassium channel and recurrent ventricular fibrillation in failing rabbit ventricles. *Circ Res*. 2011; 108:971–979. [PubMed: 21350217]
9. Grillner S. The motor infrastructure: From ion channels to neuronal networks. *Nat Rev Neurosci*. 2003; 4:573–586. [PubMed: 12838332]

10. Zaugg CE, Wu ST, Barbosa V, Buser PT, Wikman-Coffelt J, Parmley WW, Lee RJ. Ventricular fibrillation-induced intracellular Ca^{2+} overload causes failed electrical defibrillation and post-shock reinitiation of fibrillation. *J Mol Cell Cardiol.* 1998; 30:2183–2192.
11. Burashnikov A, Antzelevitch C. Reinduction of atrial fibrillation immediately after termination of the arrhythmia is mediated by late phase 3 early afterdepolarization-induced triggered activity. *Circulation.* 2003; 107:2355–2360. [PubMed: 12695296]
12. Patterson E, Lazzara R, Szabo B, Liu H, Tang D, Li YH, Scherlag BJ, Po SS. Sodium-calcium exchange initiated by the Ca^{2+} transient: An arrhythmia trigger within pulmonary veins. *J Am Coll Cardiol.* 2006; 47:1196–1206. [PubMed: 16545652]
13. Nakagawa H, Scherlag BJ, Patterson E, Ikeda A, Lockwood D, Jackman WM. Pathophysiologic basis of autonomic ganglionated plexus ablation in patients with atrial fibrillation. *Heart rhythm: the official journal of the Heart Rhythm Society.* 2009; 6:S26–34. [PubMed: 19959140]
14. Chang P-C, Turker I, Lopshire JC, Masroor S, Nguyen BL, Tao W, Rubart M, Chen PS, Chen Z, Ai T. Heterogeneous upregulation of apamin-sensitive potassium currents in failing human ventricles. *JAHA.* 2013; 1:e004713. [PubMed: 23525437]
15. Roden DM. Taking the “idio” out of “idiosyncratic”: Predicting torsades de pointes. *Pacing Clin Electrophysiol.* 1998; 21:1029–1034. [PubMed: 9604234]
16. Weiss JN, Garfinkel A, Karagueuzian HS, Chen PS, Qu Z. Early afterdepolarizations and cardiac arrhythmias. *Heart rhythm: the official journal of the Heart Rhythm Society.* 2010; 7:1891–1899. [PubMed: 20868774]
17. Nattel S, Maguy A, Le BS, Yeh YH. Arrhythmogenic ion-channel remodeling in the heart: Heart failure, myocardial infarction, and atrial fibrillation. *Physiol Rev.* 2007; 87:425–456. [PubMed: 17429037]
18. Chou CC, Zhou S, Hayashi H, Nihei M, Liu YB, Wen MS, Yeh SJ, Fishbein MC, Weiss JN, Lin SF, Wu D, Chen PS. Remodelling of action potential and intracellular calcium cycling dynamics during subacute myocardial infarction promotes ventricular arrhythmias in langendorff-perfused rabbit hearts. *J Physiol.* 2007; 580:895–906. [PubMed: 17272354]
19. Maruyama M, Joung B, Tang L, Shinohara T, On YK, Han S, Choi EK, Kim DH, Shen MJ, Weiss JN, Lin SF, Chen PS. Diastolic intracellular calcium-membrane voltage coupling gain and postshock arrhythmias: Role of Purkinje fibers and triggered activity. *Circulation Research.* 2010; 106:399–408. [PubMed: 19926871]
20. Licata A, Aggarwal R, Robinson RB, Boyden P. Frequency dependent effects on Ca^{2+} transients and cell shortening in myocytes that survive in the infarcted heart. *Cardiovascular Research.* 1997; 33:341–350. [PubMed: 9074698]
21. Schoenmakers TJ, Visser GJ, Flik G, Theuvsen AP. Chelator: An improved method for computing metal ion concentrations in physiological solutions. *Biotechniques.* 1992; 12:870–874. 876–879. [PubMed: 1642895]
22. Curran-Everett D, Benos DJ. American Physiological Society. Guidelines for reporting statistics in journals published by the American Physiological Society. *American journal of physiology. Endocrinology and metabolism.* 2004; 287:E189–191. [PubMed: 15271643]
23. Castle NA, Haylett DG, Jenkinson DH. Toxins in the characterization of potassium channels. *Trends Neurosci.* 1989; 12:59–65. [PubMed: 2469212]
24. Ishii TM, Maylie J, Adelman JP. Determinants of apamin and d-tubocurarine block in sk potassium channels. *J Biol Chem.* 1997; 272:23195–23200. [PubMed: 9287325]
25. Bkaily G, Sculptoreanu A, Jacques D, Economos D, Menard D. Apamin, a highly potent fetal I-type Ca^{2+} current blocker in single heart cells. *Am J Physiol.* 1992; 262:H463–471. [PubMed: 1539705]
26. Li W, Aldrich RW. Electrostatic influences of charged inner pore residues on the conductance and gating of small conductance Ca^{2+} activated K^{+} channels. *Proceedings of the National Academy of Sciences of the United States of America.* 2011; 108:5946–5953. [PubMed: 21422289]
27. Aiba T, Tomaselli GF. Electrical remodeling in the failing heart. *Curr Opin Cardiol.* 2010; 25:29–36. [PubMed: 19907317]
28. Huang C, Bao M, Jiang H, Liu J, Yang B, Wang T. Differences in the changing trends of monophasic action potential duration and effective refractory period of the ventricular

- myocardium after myocardial infarction in vivo. *Circulation journal: official journal of the Japanese Circulation Society*. 2004; 68:1205–1209. [PubMed: 15564708]
29. Bonilla IM, Long VL, Vargas-Pinto P, Green J, Yoo J, Allen D, Wright P, Mohler PJ, Carnes CA. Calcium-activated potassium current modulates ventricular (but not atrial) repolarization in chronic heart failure. *Circulation*. 2012; 126:A16846. (Abstract).
 30. Tsuji Y, Hojo M, Voigt N, El-Armouche A, Inden Y, Murohara T, Dobrev D, Nattel S, Kodama I, Kamiya K. Ca(2+)-related signaling and protein phosphorylation abnormalities play central roles in a new experimental model of electrical storm. *Circulation*. 2011; 123:2192–2203. [PubMed: 21555709]
 31. Hsieh Y-C, Chang P, Lee Y-S, Weiss J, Chen Z, Ai T, Lin S, Chen P-S. Inhibition of small conductance ca-activated k channels flattens the action potential duration restitution and hinders the maintenance of ventricular fibrillation in failing rabbit ventricles. *J Arrhythmia*. 2012; 28:S-098 (abstract).
 32. Ogawa M, Morita N, Tang L, Karagueuzian HS, Weiss JN, Lin SF, Chen PS. Mechanisms of recurrent ventricular fibrillation in a rabbit model of pacing-induced heart failure. *Heart Rhythm*. 2009; 6:784–792. [PubMed: 19467505]
 33. Lue WM, Boyden PA. Abnormal electrical properties of myocytes from chronically infarcted canine heart. Alterations in v_{max} and the transient outward current. *Circulation*. 1992; 85:1175–1188. [PubMed: 1371431]

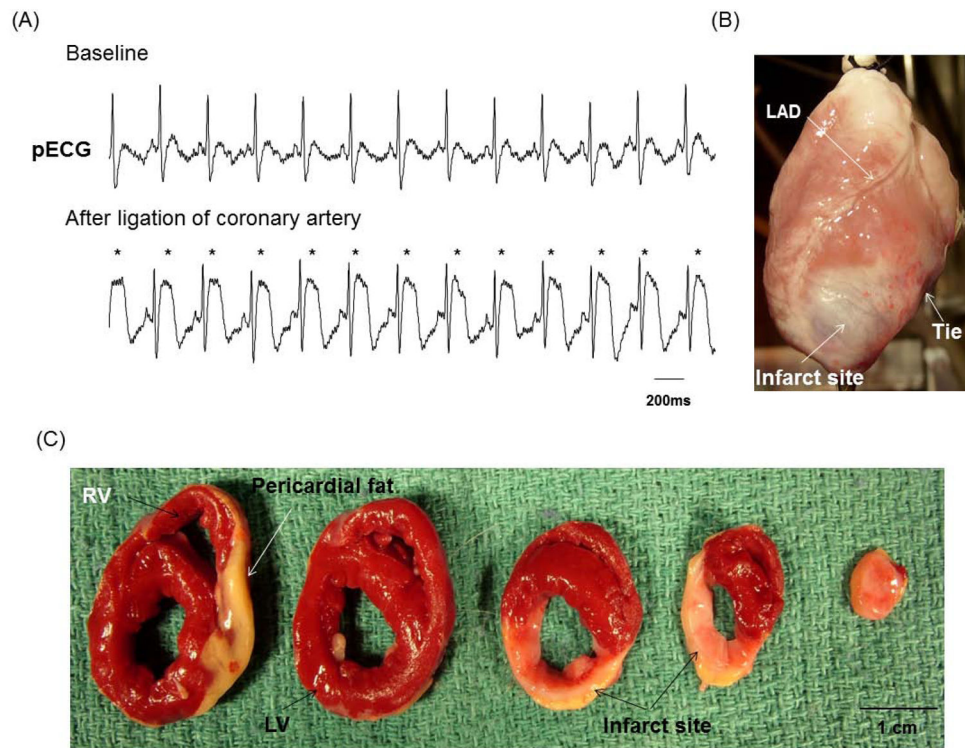


Figure 1. Creation of chronic MI. A, After ligation of coronary artery, definite ST segment elevation (asterisks) was seen on the pseudo ECG (pECG). B, Photography of the anterior view of the infarcted heart showed white fibrotic area at apex of left ventricle (LV). C, The triphenyl tetrazolium chloride staining of the infarcted heart showed brisk red for surviving myocardium and white for infarcted myocardium. LAD, left anterior descending coronary artery; RV, right ventricle.

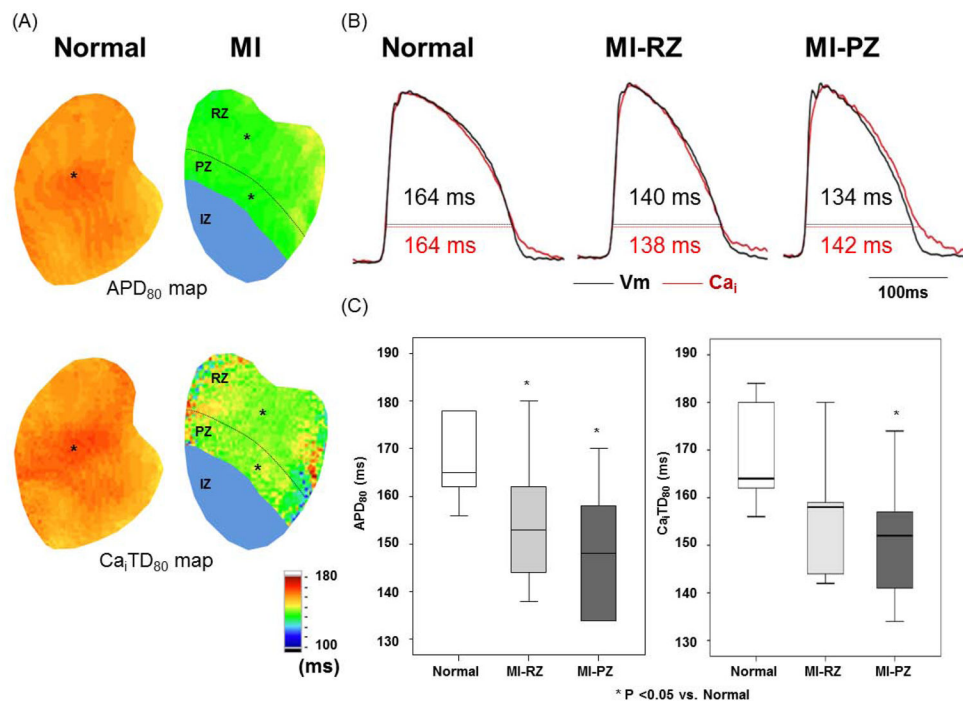


Figure 2.

Action potential duration (APD) and intracellular Ca transient duration (Ca_iTD) in normal and infarcted ventricles. Measurements were made with PCL of 300 ms in 6 normal and 7 infarct ventricles. A, APD₈₀ map and Ca_iTD₈₀ map obtained from normal and infarcted ventricles. We divided MI ventricle to three regions. The infarct zone (IZ) has the region distal to coronary ligation. The peri-infarct zone (PZ) was defined as the region within one-third of the distance from the edge of the infarct. The remaining two-thirds of the non-infarcted region was the remote zone (RZ). B, Black and red lines indicate optical tracings of V_m and intracellular calcium (Ca_i), respectively. The optical tracings were recorded from the site labeled by an asterisk in the APD₈₀ map and Ca_iTD₈₀ map in A. C, Average of APD₈₀ and Ca_iTD₈₀ at fixed PCL of 300 ms in normal (N=6) and RZ (N=7) and PZ (N=7). Boxplots were used to compare the median and the range of the data associated with normal ventricles, MI-RZ and MI-PZ. APD₈₀ and Ca_iTD₈₀ indicate APD and Ca_i transient duration, respectively, measured at 80% repolarization.

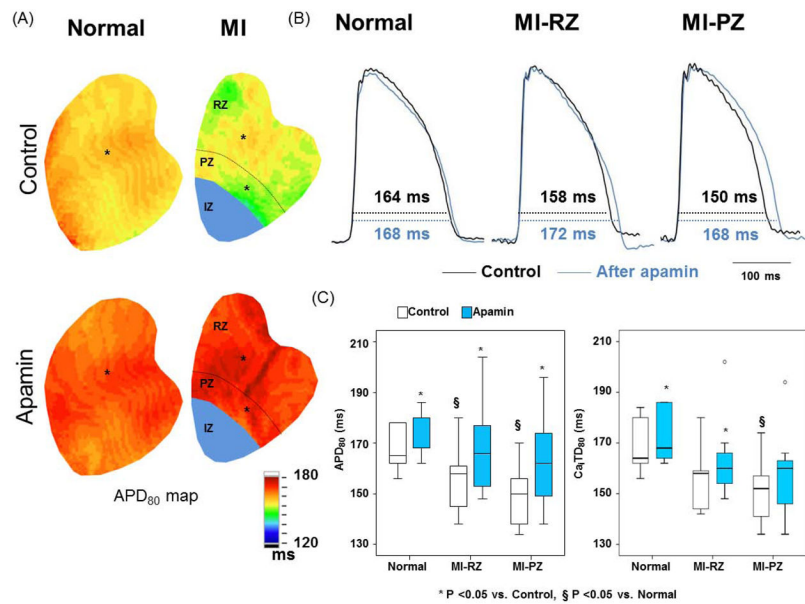


Figure 3.

Effects of apamin on APD₈₀ and Ca_iTD₈₀ in normal and infarct ventricles. A, Typical APD₈₀ maps before and after apamin in normal and infarct ventricles. B, Black and blue lines indicated the optical Vm tracing before and after application of apamin, respectively. The tracings were obtained from the site labeled by an asterisk in A. C, Magnitude of APD₈₀ (left panel) and Ca_iTD₈₀ (right panel) prolongation before and after apamin in 6 normal and 7 infarct ventricles. Paired t tests show significant prolongation of Ca_iTD₈₀ before (control) and after adding apamin.

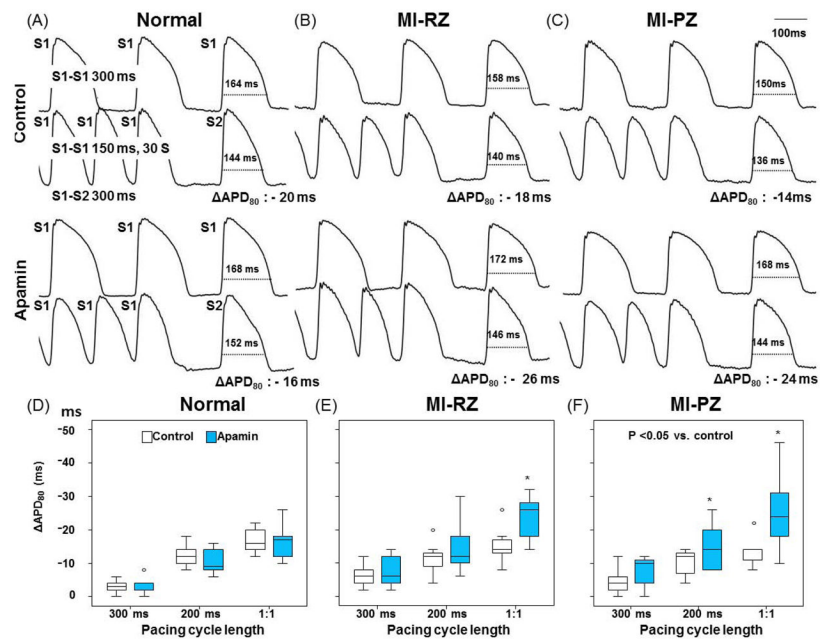


Figure 4.

Effects of apamin on action potential duration (APD) at the cessation of rapid pacing. In A through C, the first and third rows show action potential at PCL of 300 ms followed by S2 with S1–S2 of 300 ms. The second and fourth rows show APs during rapid pacing followed by a postpacing (S2) beat at 300 ms coupling interval. The difference between APD₈₀ of S2 and that of S1 at 300 ms PCL is the ΔAPD_{80} . The same pacing protocol was performed before and after apamin. D and F show effect of apamin on ΔAPD_{80} of each pacing cycle length in normal, MI-RZ and MI-PZ, respectively. 1:1 indicates the shortest PCL associated with 1:1 capture. The average shortest PCL associated with 1:1 pacing in normal and MI ventricles were 153.3 [95% CI, 144.8 to 161.9] ms and 161.4 [95% CI, 150.2 to 172.7] ms, respectively (P=0.194). The asterisk indicates p<0.05 between control and apamin at each PCL.

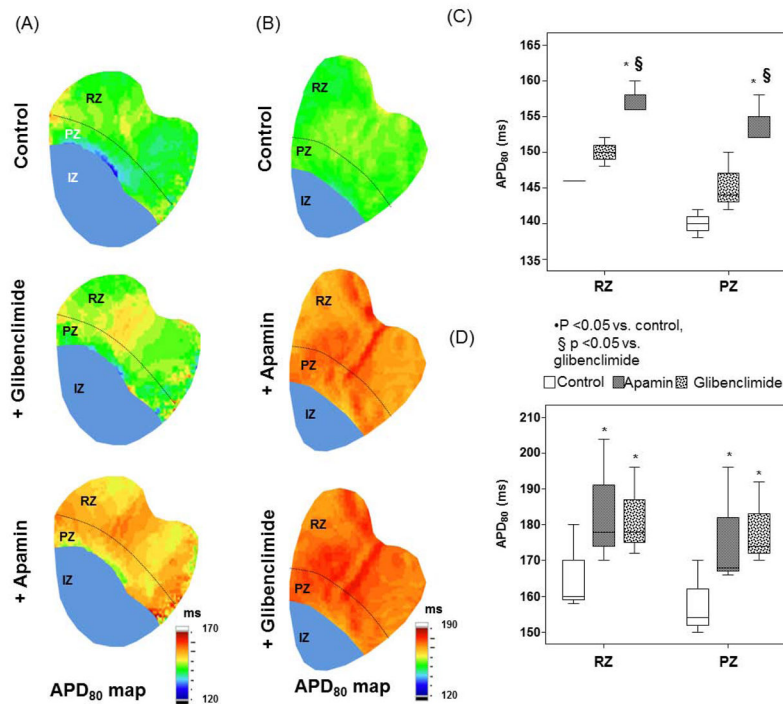


Figure 5.

Effects of glibenclamide given on action potential duration (APD₈₀). A shows the APD₈₀ distribution at baseline control, after adding glibenclamide (middle panel) and finally after adding apamin (bottom panel) in a typical example. C shows the box plot of the values throughout the mapped region. Note that there were no significant differences of APD₈₀ between control and glibenclamide, but APD₈₀ lengthened significantly after apamin was added. B shows the APD₈₀ distribution at baseline, after apamin (middle panel) and after both apamin and glibenclamide (bottom panel). D shows the box plot of the values throughout the mapped region. Note that the APD₈₀ prolonged significantly after adding apamin, but no further prolongation was noted when glibenclamide was added. The infarcted or ischemic epicardial areas were marked by blue color. They were excluded from the analyses.

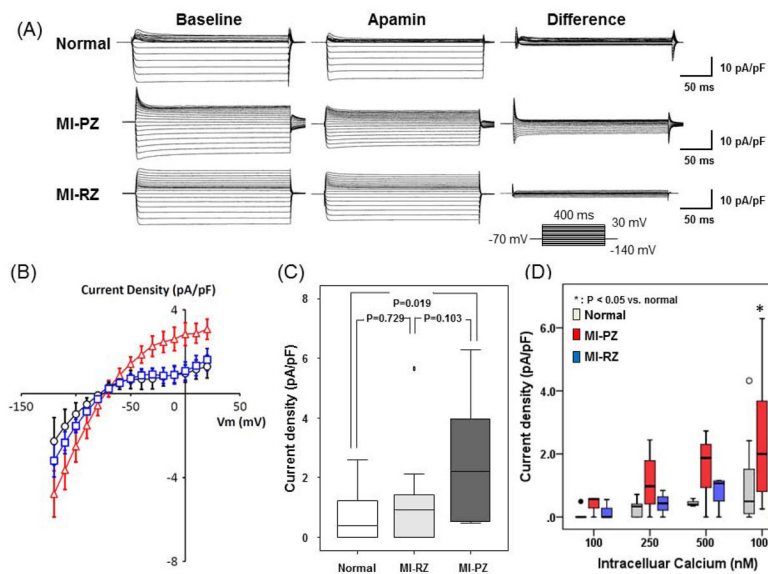


Figure 6.

Patch clamp studies of apamin-sensitive K⁺ currents (I_{KAS}) in chronic MI. A, Representative K⁺ current traces obtained from normal, MI peri-infarct zone (MI-PZ) and MI remote zone (MI-RZ) ventricular myocytes. Voltage-pulse protocol is shown in the inset. “Baseline” shows current traces in the absence of apamin ($I_{baseline}$); Apamin indicates the use of 100 nmol/L apamin in bath solution (I_{apamin}); “Difference” shows I_{KAS} calculated as $I_{baseline} - I_{apamin}$. B, I-V curve of I_{KAS} from MI-PZ (red), MI-RZ (blue) and normal (black) ventricular cells. C, I_{KAS} density at 0 mV recorded from epicardial cells of normal, RZ-MI and PZ-MI. There was higher I_{KAS} density in MI-PZ than that of MI-RZ and normal cells. D, I_{KAS} and Ca_i concentration. Asterisk indicates that the I_{KAS} is significantly ($p=0.02$) higher in the MI-PZ than MI-RZ and normal control at 1,000 nM Ca_i concentration.